

Point Vortices in a Periodic Box

MAKOTO UMEKI*

*Department of Physics, Graduate School of Science, University of Tokyo,
7-3-1 Hongo, Bunkyo-ku, Tokyo, 113-0033 Japan*

A motion of point vortices with periodic boundary conditions is studied by using Weierstrass zeta functions. Scattering and recoupling of a vortex pair by a third vortex becomes remarkable when the vortex density is large. Clustering of vortices is examined by a probability distribution of velocity circulation of circles in the two-dimensional flow.

KEYWORDS: point vortex, two-dimensional turbulence, *Mathematica*

A statistical approach to a problem of assemblies of point vortices (PVs) goes back to Onsager (1949). A state of negative temperature is considered to be related to clustering of vortices rotating in the same direction and the inverse energy cascade predicted in the two-dimensional Navier-Stokes (2D NS) turbulence. In many numerical simulations, PVs are bounded in a circular wall, since a velocity field due to a PV can be computed by including a single mirror image. Although the axisymmetry with respect to the origin is conserved, the spatial homogeneity is not guaranteed in such a circular system. There has been a numerical difficulty in a simulation of vortices in a box that there emerges an infinite sequence of mirror images. Stremler and Aref (1999)¹ applied a passive particle method and showed the complicated motions of three PVs in a periodic parallelogram. Our objective is to study such turbulent motions of many PVs in a periodic box using Weierstrass elliptic functions and *Mathematica*.

Let us start by representing the 2D NS equation in terms of a complex position $z = x + iy$, velocity $q = u - iv$, pressure p and the kinematic viscosity ν as

$$q_t + qq_{\bar{z}} + \bar{q}q_z = -2p_z + 4\nu q_{z\bar{z}}. \quad (1)$$

Here, \bar{q} denotes the complex conjugate of q and we use the relations $\partial_x = \partial_z + \partial_{\bar{z}}$, $\partial_y = i(\partial_z - \partial_{\bar{z}})$, $u = (q + \bar{q})/2$, $v = i(q - \bar{q})/2$ and $\Delta = 4\partial_{z\bar{z}}$. The incompressible condition gives

$$\nabla \cdot \mathbf{v} = u_x + v_y = \bar{q}_z + q_{\bar{z}} = 0. \quad (2)$$

The vorticity $\omega = v_x - u_y$ can be expressed by q as

$$\omega = 2iq_{\bar{z}}. \quad (3)$$

If the flow is irrotational $\omega = 0$, then $q_{\bar{z}} = 0$, q depends on only z (and t) and theory of

*E-mail address: umeki@phys.s.u-tokyo.ac.jp

conformal mapping can be applied. Equations for the vorticity and pressure are respectively

$$q_{\bar{z}t} + qq_{\bar{z}\bar{z}} + \bar{q}q_{z\bar{z}} = 4\nu q_{z\bar{z}\bar{z}}, \quad (4)$$

and

$$p_{z\bar{z}} = -(q_z \bar{q}_{\bar{z}} + \bar{q}_z^2)/2. \quad (5)$$

According to Tkachenko,^{2,3} the velocity field due to a single PV at the origin with periodic boundary conditions (BCs) is equivalent to that due to PVs on the lattice $z_{mn} = 2m\omega_1 + 2n\omega_2$, where the complex numbers ω_1, ω_2 are the half periods of the lattice and m, n are arbitrary integers. The ratio of two periods $\tau = \omega_1/\omega_2$ can be restricted in the region

$$\text{Im}\tau > 0, \quad |\text{Re}\tau| < 1/2, \quad |\tau| \geq 1. \quad (6)$$

We concentrate on the case of square periodic BCs, which is usually adapted for numerical studies of the two-dimensional turbulence by a choice of $\tau = i$. However, we can deal with an arbitrary periodic parallelogram by considering various values of τ satisfying the condition (6).

The velocity field due to a PV of strength $\kappa = 2\pi$ is given by the Weierstrass zeta function $\zeta(z; \omega_1, \omega_2)$ along with a rigid rotation term as follows:

$$\bar{q} = i\overline{\zeta(z)} - i\Omega z \equiv w(z). \quad (7)$$

Since the vortex lattice undergoes rigid rotation with angular velocity Ω given by

$$\Omega = \pi/[4\text{Im}(\bar{\omega}_1\omega_2)], \quad (8)$$

the second term in Eq.(7) is necessary in order to cancel the rotation on the boundary. The vortex density $n = 1/[4\text{Im}(\bar{\omega}_1\omega_2)]$, the angular velocity Ω and the vortex strength κ are related as

$$\kappa n = 2\Omega. \quad (9)$$

If the length of the side of the square is unit, then $\omega_1 = 1/2$, $\omega_2 = i/2$, $\Omega = \pi$ and the vortex strength κ becomes 2π .

The equation for the streamline $\psi = \text{const.}$, where ψ is the streamfunction, is equivalent to $dx/\psi_y = -dy/\psi_x$. Using the relations $u = \psi_y$ and $v = -\psi_x$, ψ is expressed as

$$\psi = \int u dy + f(x). \quad (10)$$

The sigma and zeta functions of Weierstrass are related as

$$\zeta = \frac{\sigma'(z)}{\sigma(z)}. \quad (11)$$

The above relation is consistent with the asymptotic forms $\zeta \sim 1/z$ and $\sigma \sim z$ when $z \sim 0$. Using the sigma function and (10), ψ for a single vortex lattice centered at the origin is given

by

$$\psi = -\text{Re} \ln \sigma + \frac{\Omega}{2} |z|^2. \quad (12)$$

A pattern of the streamfunction (12) and its values on the real axis $z = x$ are plotted in Figure 1a and 1b, respectively, for $(\omega_1, \omega_2) = (1/2, i/2)$ and $\Omega = \pi$.

For an assembly of PVs, we consider the case $\kappa_i = 2\pi\mu_i$, $\mu_i = 1, i = 1, \dots, N_1$ and $\mu_i = -1, i = N_1 + 1, \dots, N (= N_1 + N_2)$ for simplicity. Therefore, the streamfunction for N vortices located at z_i is given by

$$\psi = \sum_{i=1}^N \mu_i \{-\text{Re}[\ln \sigma(z - z_i)] + \frac{\Omega}{2} |z - z_i|^2\}. \quad (13)$$

Using Eq. (7), the equation of motion of PVs with square periodic BCs can be expressed as

$$\frac{dz_i}{dt} = \sum_{j \neq i} \mu_j w(z_i - z_j). \quad (14)$$

The equation can be rewritten in Hamiltonian form as

$$\mu_i \frac{dz_i}{dt} = \frac{\partial H}{\partial \bar{z}_i}, \quad (15)$$

where the Hamiltonian H can be expressed as

$$H = \sum_{i=1}^N \mu_i h_i = \sum_{i=1}^N \sum_{j=1, j \neq i}^N \mu_i \mu_j h_{ij}, \quad (16)$$

$$h_{ij} = -\text{Re}[\ln \sigma(z_i - z_j)] + \frac{\Omega}{2} |z_i - z_j|^2. \quad (17)$$

From the above expression, the Hamiltonian, which is a total kinetic energy minus self induced kinetic energy of vortices, can be interpreted as a sum of kinetic energy due to an interaction between pairs of vortices.

If *Mathematica* is used, we can compute the Weierstrass zeta function as we use the sinusoidal function in a Fortran code. The system (7,14) is solved numerically by the *NDSolve* of *Mathematica* 5.2 installed in the PC having an AMD Athlon 64x2 3800 CPU, 2GB memory and Windows XP OS. The computation is realistic since the CPU time in such a PC environment is order of two days for 100 PVs and 10 eddy turnover times and the relative precision of the conserved quantities is tolerable, as described below.

If PVs lie in an unbounded domain, the system has four integrals,⁴ the Hamiltonian $H_u = -\sum \mu_i \mu_j \ln |z_i - z_j|$, two components of the linear impulse $\mathbf{I} = (I_x, I_y)$, $I_x = \sum \mu_i \text{Re}[z_i]$, $I_y = \sum \mu_i \text{Im}[z_i]$, and the angular impulse $A = \sum \mu_i |z_i|^2$. Since the system in a periodic box has no circular symmetry, A is no more constant, but H , I_x , and I_y remains to be conserved. Since there are three conserved quantities, the system of three vortices is integrable, while the four vortices show chaotic motions.

Examples of trajectories of three vortices $\kappa_i = 2\pi\mu_i$, $\mu_i = (2, 2, -1)$ with an initial con-

dition $(z_1, z_2, z_3) = (0, 0.5, 0.25 + i\sqrt{3}/4)$ located at the vertices of a triangular, and of four vortices $\mu_i = (2, 2, -1, -1)$ and $(z_1, z_2, z_3, z_4) = (0, 0.5, i\sqrt{3}/4, 0.5 + i\sqrt{3}/4)$ at $t = 0$ located as a square, are given in Figure 2a and 2b, respectively.

Another example is a numerical simulation of a vortex sheet. PVs of the same strength 2π are located initially on a curve slightly deviating from the x-axis;

$$z_j(0) = j/N + i\epsilon \sin 2\pi j/N, \quad j = 1, \dots, N. \quad (18)$$

The simulation is done with $N = 100$ and $\epsilon = 0.02$. If ϵ is fixed and N is increased, pairing of two adjacent vortices becomes more conspicuous than the winding of the sheet due to the Kelvin-Helmholtz instability. Figure 3 shows contours of ψ and the location at $t = 0.001$ and 0.002 . The contour plot is comparable with those obtained in the two-dimensional Navier-Stokes simulation, although the plot of PVs reminds us the possibility of the singularity of the vortex sheet.

Finally we show a numerical result of a simulation of 100 PVs ($N_1 = N_2 = 50$) which are initially located randomly. The relative precision of H is confirmed to be less than 10^{-6} up to the final time $t = 0.1$. Figure 4 shows the distributions of PVs and the contours of ψ at $t = 0$ and $t = 0.1$.

A remarkable feature in this turbulent situation is that there are several pairs of a positive and negative vortex moving linearly at a velocity $\kappa/4h\pi$, where $2h$ is a distance of two vortices. Since the pair is surrounded by a number of other isolated vortices, however, the moving direction is bent by a third vortex when they pass each other. Moreover, if the collision is nearly head-on, a vortex of the pair with the opposite sign of the third target vortex replaces its partner by the latter and then continues to move linearly again. An exact analysis of such scattering of three vortices in an unbounded domain was already given in Appendix of Aref (1979)⁵ using elliptic integrals.

Examples of scattering and recoupling of three vortices in a periodic box are given by an initial location $(z_1, z_2, z_3) = (L + iL, (L + d + h)i, (L + d - h)i)$ with $L = 1/2$. A pair of vortex 2 and 3 is approaching vortex 1 initially. Figure 5 shows their trajectories in the cases $h = 0.02$ and $d = \pm 0.02, \pm 0.01, 0.04, 0.08, 0.16$ and 0.32 . The final time t_f is 0.04 except for $t_f = 0.1$ for $d = 0.16$, $t_f = 0.05$ for $d = 0.32$ and $t_f = 0.06$ for $d = -0.01$. Recoupling is observed for $d = 0.01, 0.02, 0.04, 0.08$ and 0.16 . Corresponding to Figure 11 in Aref (1979),⁵ the dependence of a π -normalized scattering angle $\delta\phi/\pi$ measured by the moving direction of $z_3(t = 0.04)$ for $h = 0.02$ in a periodic box is shown in Figure 6. The recoupling of vortices in an unbounded plane with $L \rightarrow \infty$ ⁵ occurs if

$$0 < d/h < 9. \quad (19)$$

On the other hand, the present simulation in a periodic box with $h = 0.02$ shows a shift of

the range d for recoupling as

$$-0.01 \lesssim d \lesssim 0.17. \quad (20)$$

In a GIF animation made by the numerical simulation of $N_1 = N_2 = 50$ PVs, successive scattering and recoupling, similar to chaos in the billiard system, are clearly observed. An existence of such vortex pairs may play a crucial role of stirring assemblies of vortices. Iterations of scattering is revealed in Figure 7, showing a trajectories of a positive vortex having the shortest distance to a negative vortex. A longer distance between dots located on lines denotes a larger velocity. The time step is 10^{-4} and 10^3 points are plotted in Fig. 7. The linear movement of a vortex pair may be closely related to the filamentation of a vortex patch observed in the numerical simulation of the 2D NS turbulence.

Since an average distance of randomly located PVs is $l \sim N^{-1/2}$ and the strength is fixed 2π , a typical velocity and eddy turnover time is respectively $v \sim N^{1/2}$ and $t_e \sim 1/N$. Denoting the smallest distance of the vortex pair by αl , its velocity is $V \sim 1/\alpha l$. Because of the recoupling condition (19), the cross section of the scattering is about $\sigma_c \sim d \sim 10\alpha l$ and the area swept by the pair during t_e is $S \sim dVt_e \sim 10/N$. Therefore the condition for the scattering to occur in t_e is $N \sim 10$ since $S \sim 1$, the size of the square. If $N = 100$, $t_e \sim 0.01$ and approximately one pair will be scattered ten times in a numerical simulation in the time interval $0 \leq t \leq 0.1 \sim 10t_e$.

In order to examine clustering of PVs, the probability distribution function (PDF) of velocity circulation is investigated, which is studied in Umeki (1993)⁶ in three-dimensional turbulence motivated by Professor Migdal's work.⁷ If PVs of strength 2π are randomly distributed in a square of unit length, which is the case of the initial condition, the velocity circulation along a circles of radius r ($0 < r < 1/2$) is $2m\pi(1 - \pi r^2)$, where $m = m_1 - m_2$ is an integer, m_1 (m_2) is a number of PVs of positive (negative) strength, and the term r^2 is due to the rigid rotation. The probability for $m \geq 0$ is

$$P_r(m; r) = \sum_{m_1=m}^{N_1} {}_{N_1}C_{m_1} {}_{N_2}C_{m_1-m} (\pi r^2)^{2m_1-m} (1 - \pi r^2)^{N-2m_1+m} \quad (21)$$

However, if clustering of PVs occurs, the configuration of PVs will deviate from Eq. (21) and the probability becomes larger for nonzero m . Since clustering is considered to form a larger eddy, the deviation will be remarkable at a large r , which is contrary to the normal cascade in three-dimensional turbulence.⁶

Figure 8 shows the PDF of velocity circulation $2m\pi(1 - \pi r^2)$ along a circle of radius $r = 1/3$ by counting a number $m = m_1 - m_2$ for a random distribution given by Eq. (21), the exponential distribution, and the numerical data of the initial and final states $t = 0$ and 0.1 . Sampling is made at 20×20 circles centered at square lattices. The final state has a tendency of a larger probability for $4 \leq |m| \leq 10$ than the initial random state.

In summary, a method to simulate motions of point vortices with periodic boundary conditions using *Mathematica* is described. Numerical examples of quasi-periodic, chaotic and turbulent motions of PVs with N from 3 to 100 are shown and clustering of PVs are examined by the PDF of velocity circulation in the two-dimensional flow.

The author is grateful to Professor Yamagata for support of his research on fluid dynamics during these several years.

Figure Caption

Figure 1. A pattern of the streamfunction $\psi(z)$ given by Eq. (12) for the single vortex in a periodic box (a) and its value plotted by a solid curve on the real axis $z = x$, compared with $-\log|z|$ in an unbounded plain denoted by a dashed curve (b).

Figure 2. Trajectories of three (a) and four vortices system (b). Vortices 1, 2, 3 and 4 are denoted by a solid, dashed, dotted and dotted-dashed curve, respectively.

Figure 3. A distribution (a) [(c)] of PVs and contours of the streamfunction (b) [(d)] at $t = 0.001$ [0.002]. The initial condition is a sinusoidal curve slightly deviated from the x-axis.

Figure 4. A distribution (a) [(c)] of PVs and contours of the streamfunction (b) [(d)] at $t = 0$ [0.1]. Black (gray) dots denote positive (negative) PVs. The seed for random numbers used in the *Mathematica* program is 527111.

Figure 5. Trajectories of three scattering and recoupling vortices for $h = 0.02$ and $d = \pm 0.02, \pm 0.01, 0.04, 0.08, 0.16$ and 0.32 . Thin, thick and dashed curves denote z_1 , z_2 and z_3 respectively.

Figure 6. A π -normalized scattering angle $\delta\phi/\pi$ versus d for 0.02.

Figure 7. Trajectories of a positive vortex having the shortest distance to a negative vortex, showing scattering of the most active vortex pair by a third vortex.

Figure 8. The probability distribution of velocity circulation of circles with radius $r = 1/3$. Crosses, a dashed curve, squares and circles denote the random distribution (21), the exponential function $0.5 a \exp[-|m|/a]$ with $a = 3$, numerical results at $t = 0$ and $t = 0.1$, respectively.

References

- 1) M. A. Stremler and H. Aref, *J. Fluid Mech.* **392** (1999) 101.
- 2) V. K. Tkachenko, *Sov. Phys. J.E.T.P.* **22** (1966) 1282.
- 3) V. K. Tkachenko, *Sov. Phys. J.E.T.P.* **23** (1966) 1049.
- 4) P. G. Saffman, *Vortex Dynamics* (Cambridge University Press) (1992) Chap. 7.
- 5) H. Aref, *Phys. Fluids* **22** (1979) 393.
- 6) M. Umeki, *J. Phys. Soc. Jpn.* **62** (1993) 3788.
- 7) A. A. Migdal, *Int. J. Mod. Phys.* **A10** (1994) 1197.

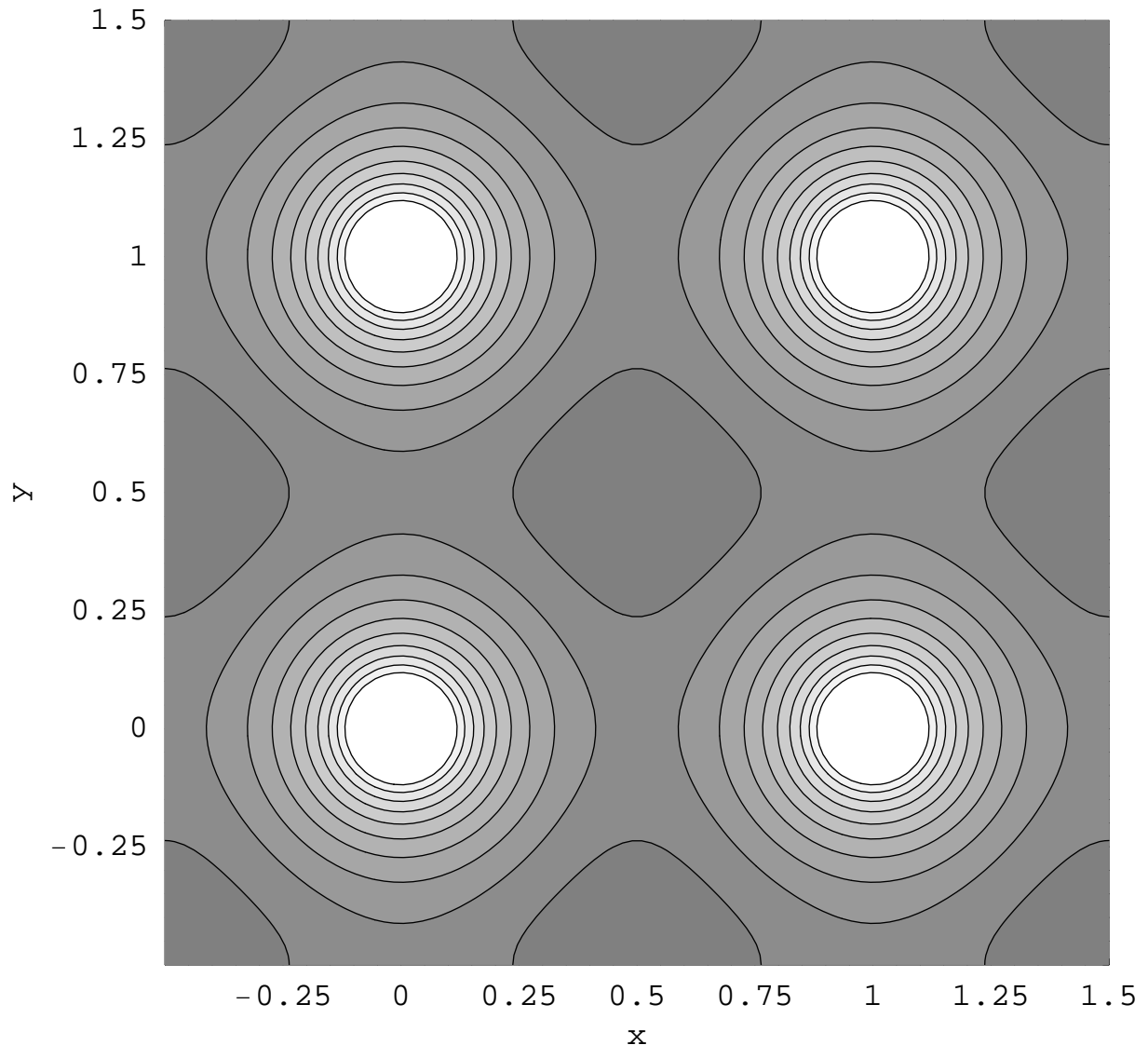


Figure 1a

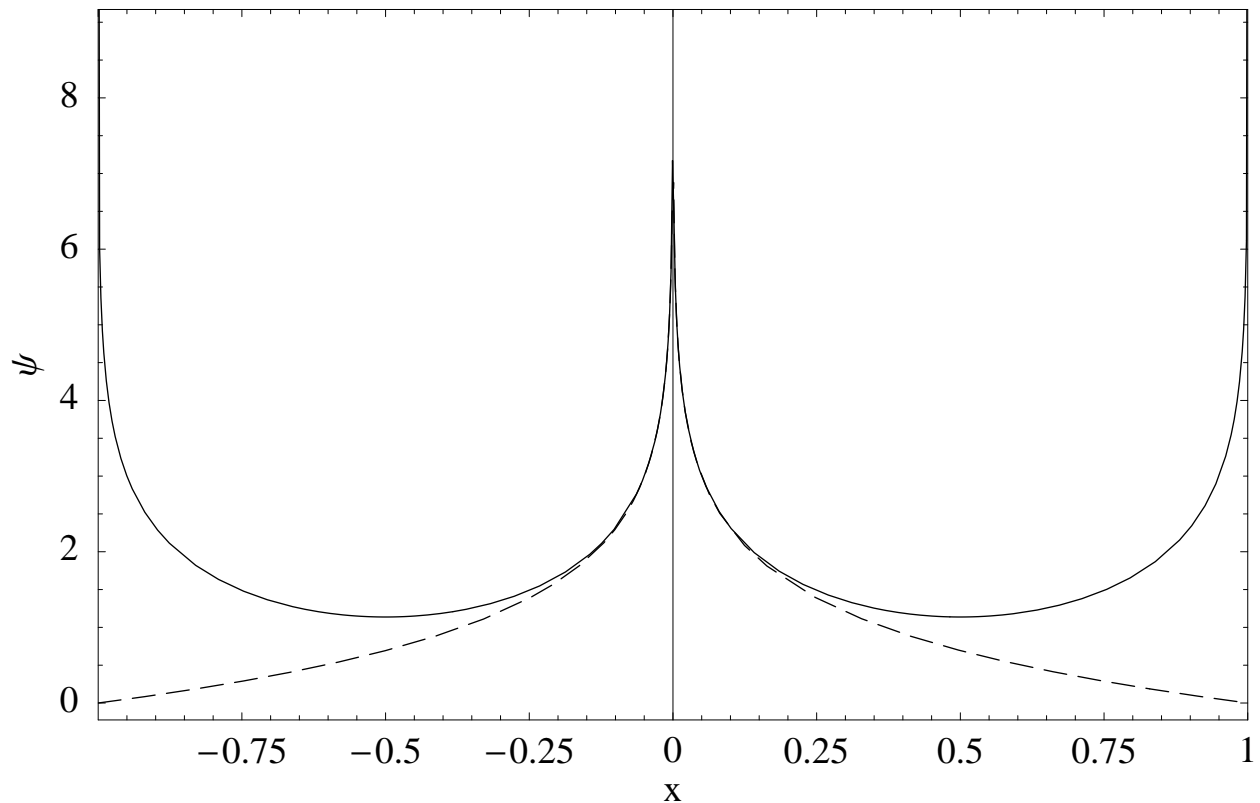


Figure 1b

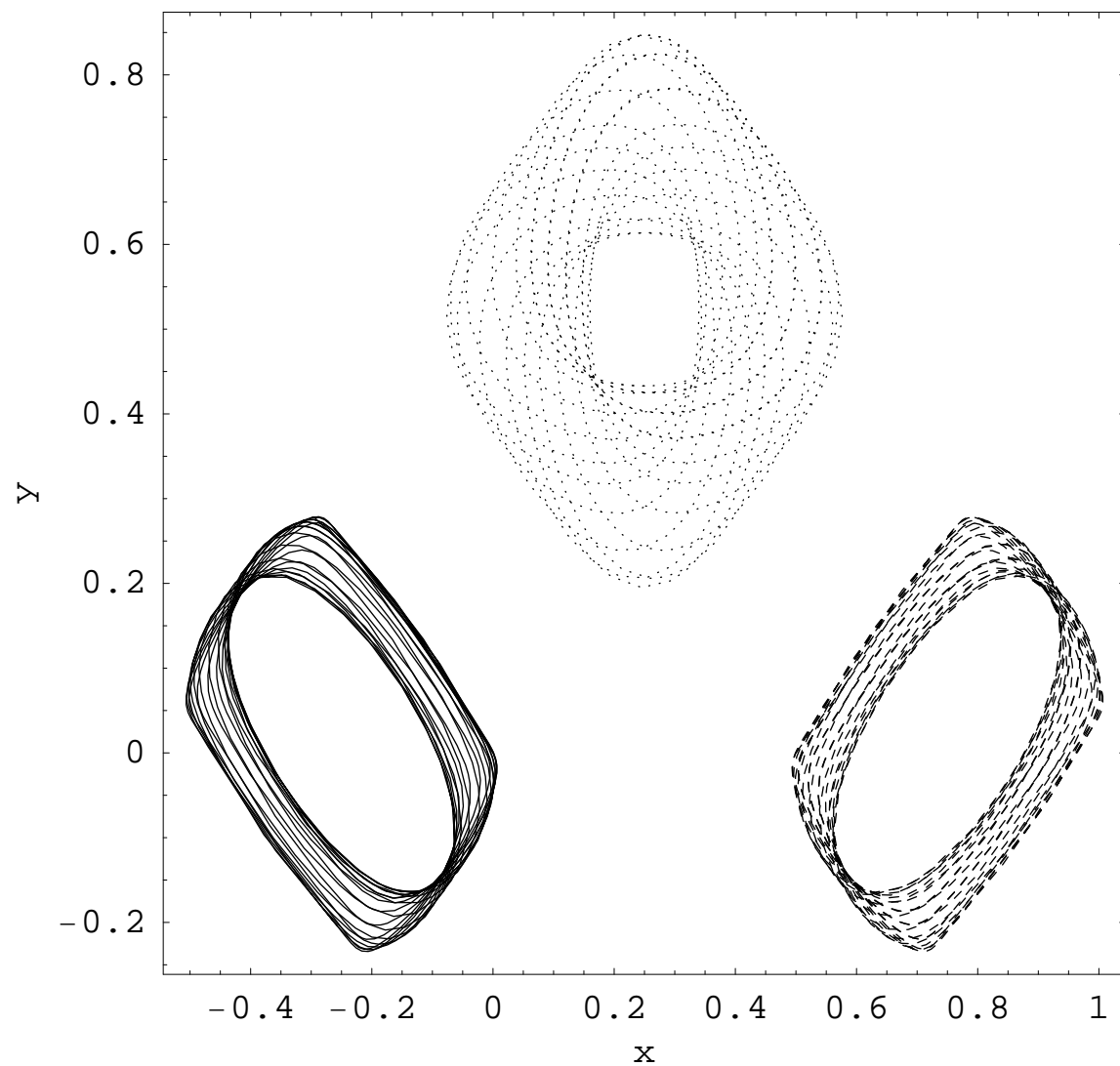


Figure 2a

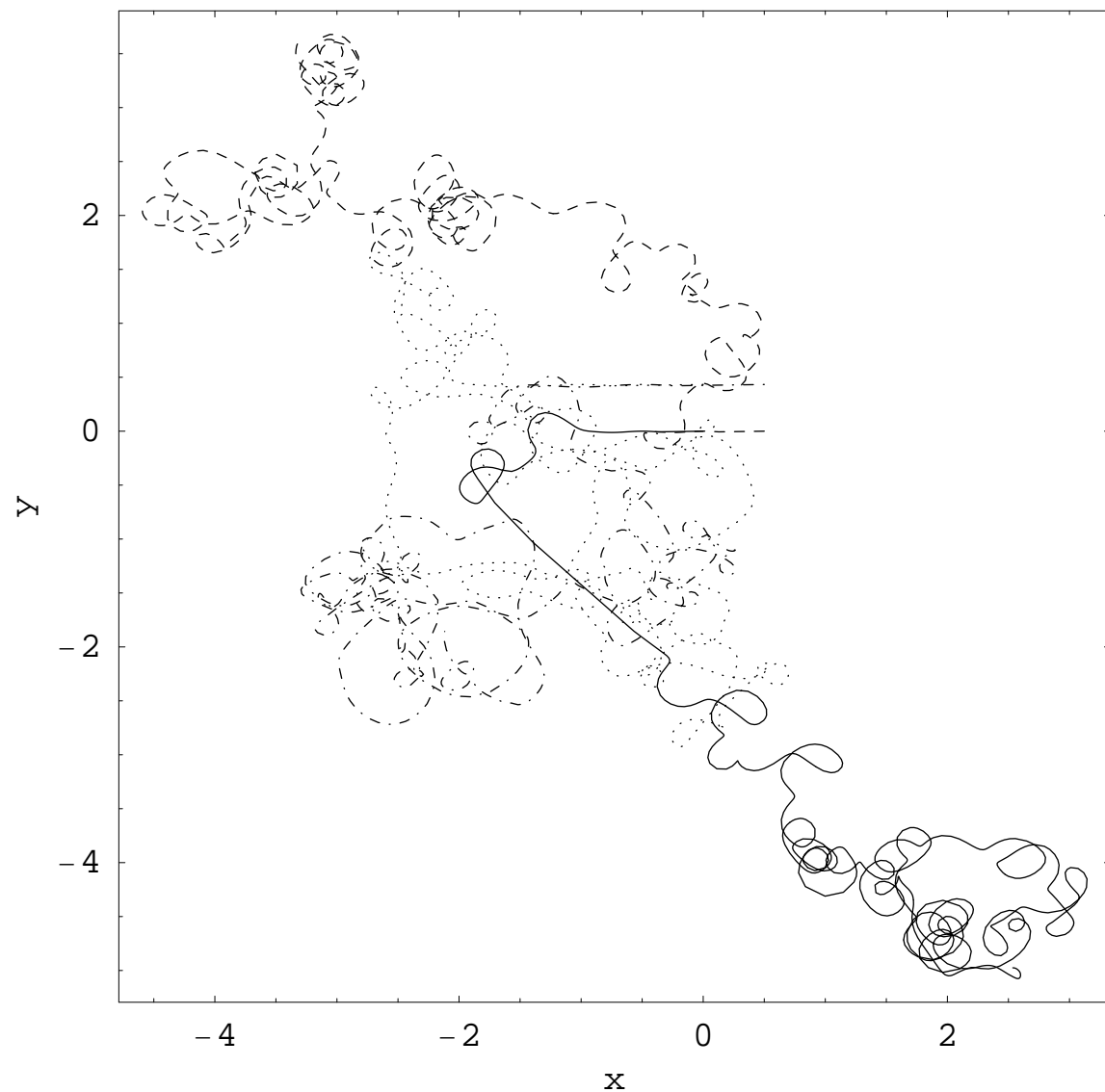


Figure 2b

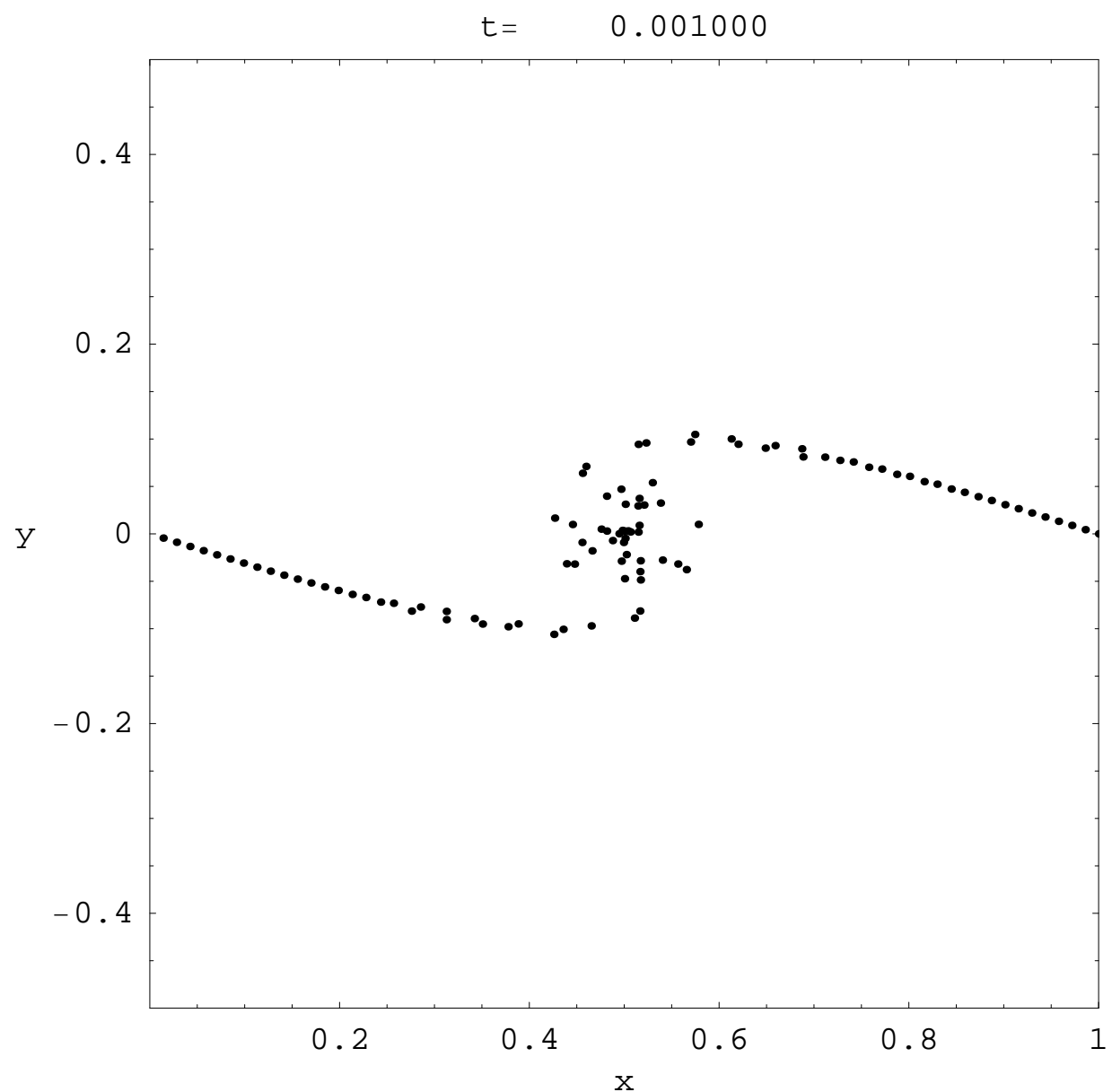


Figure 3a

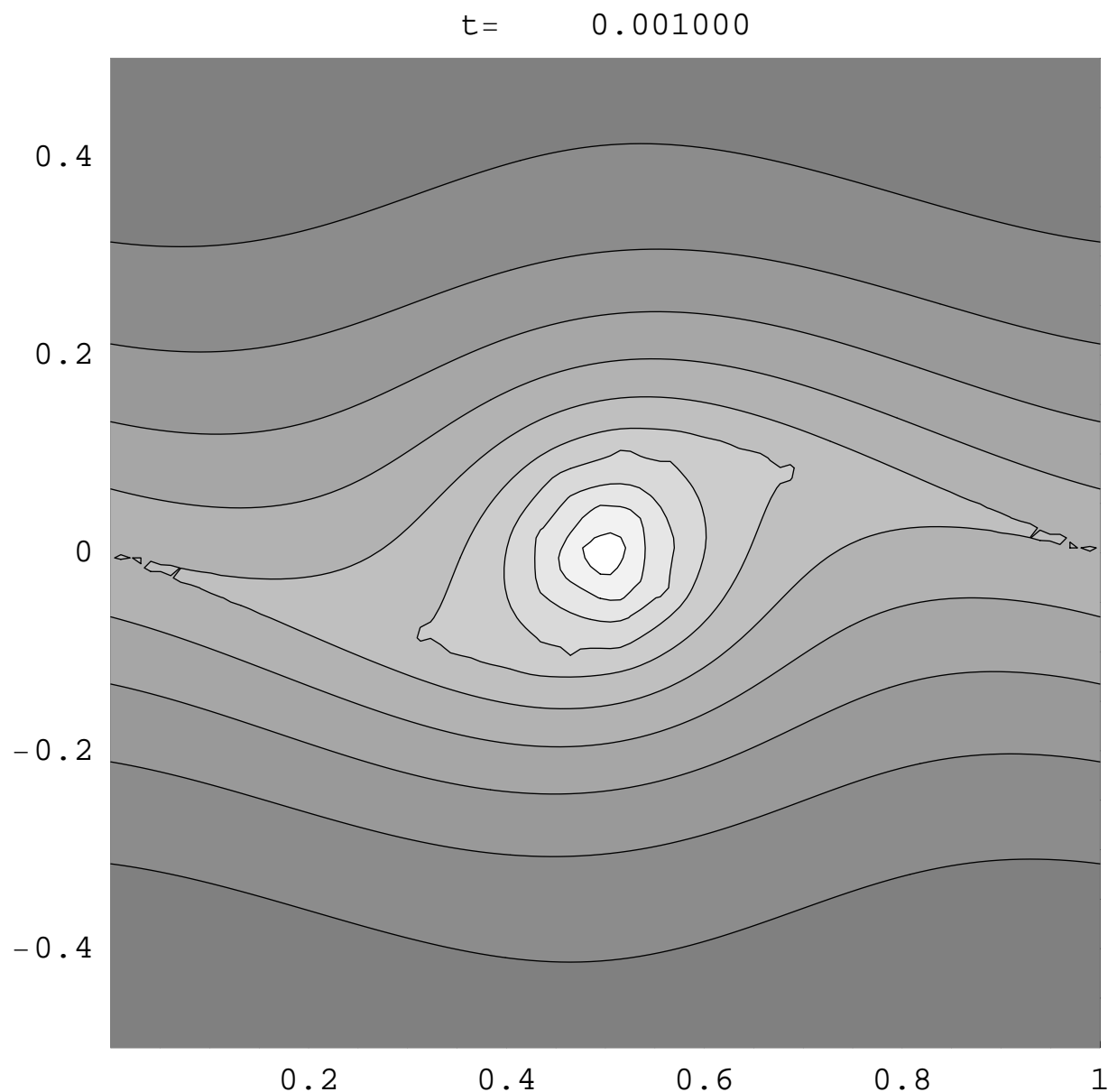


Figure 3b

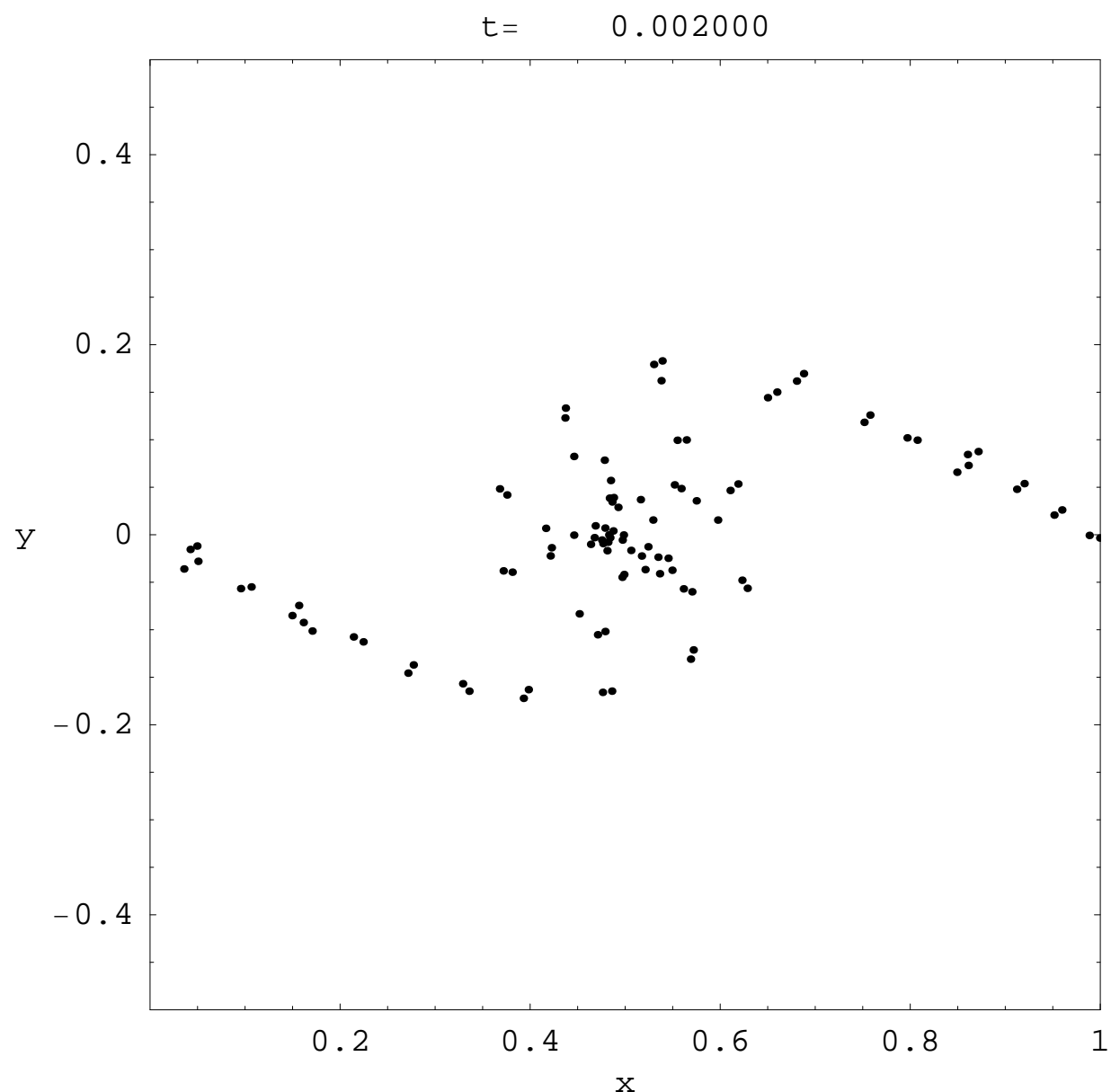


Figure 3c

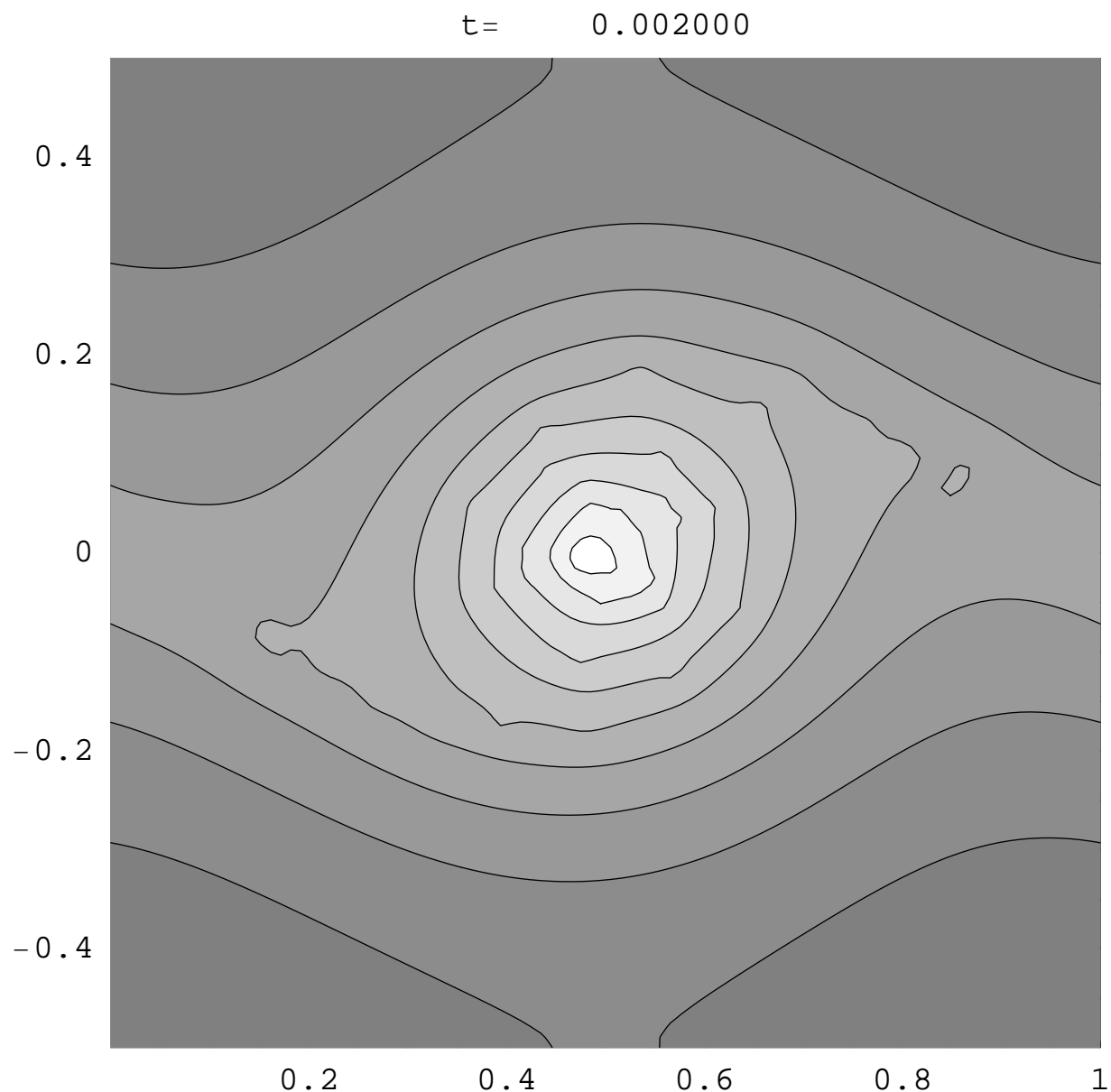


Figure 3d

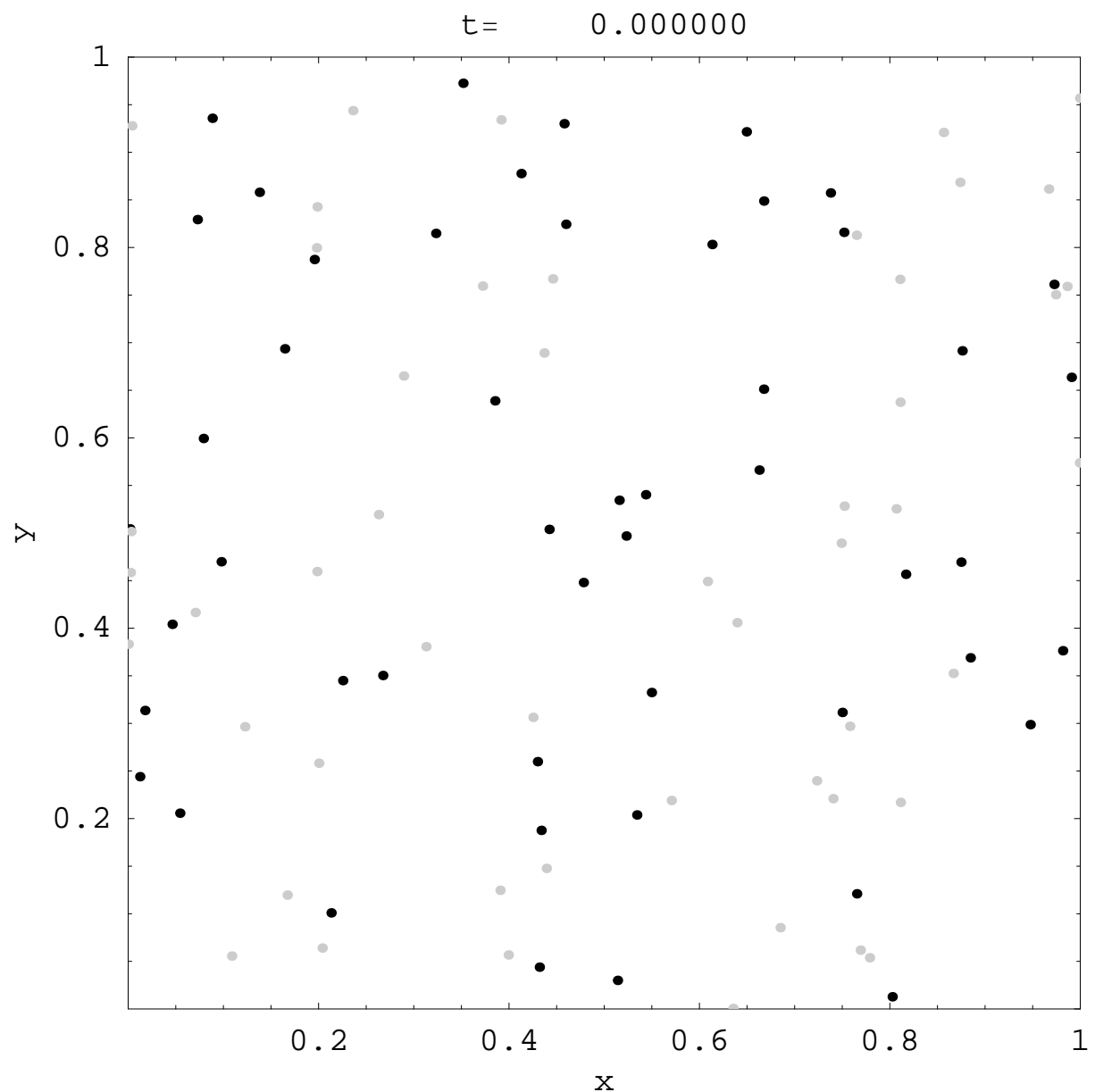


Figure 4a

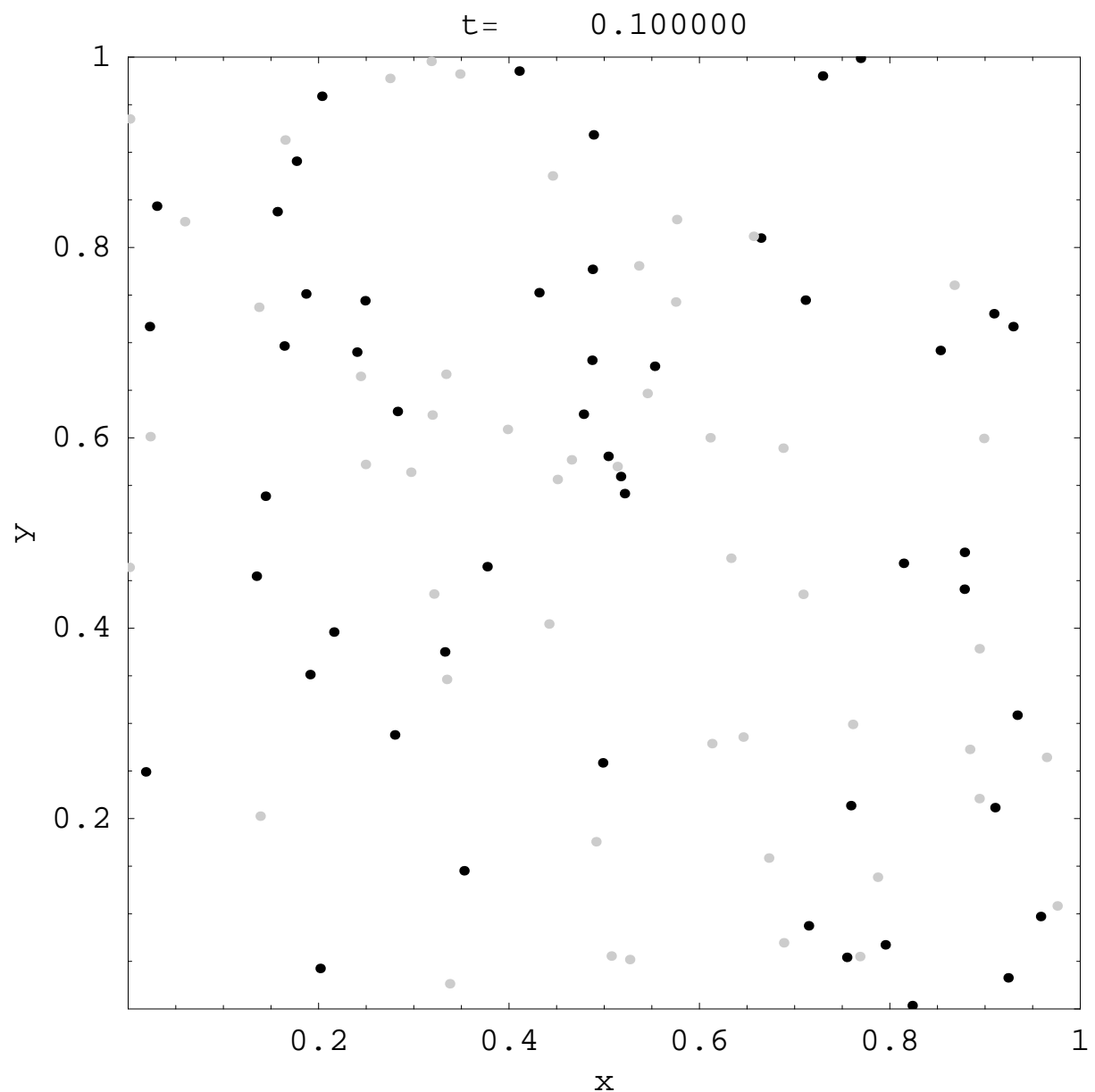


Figure 4b

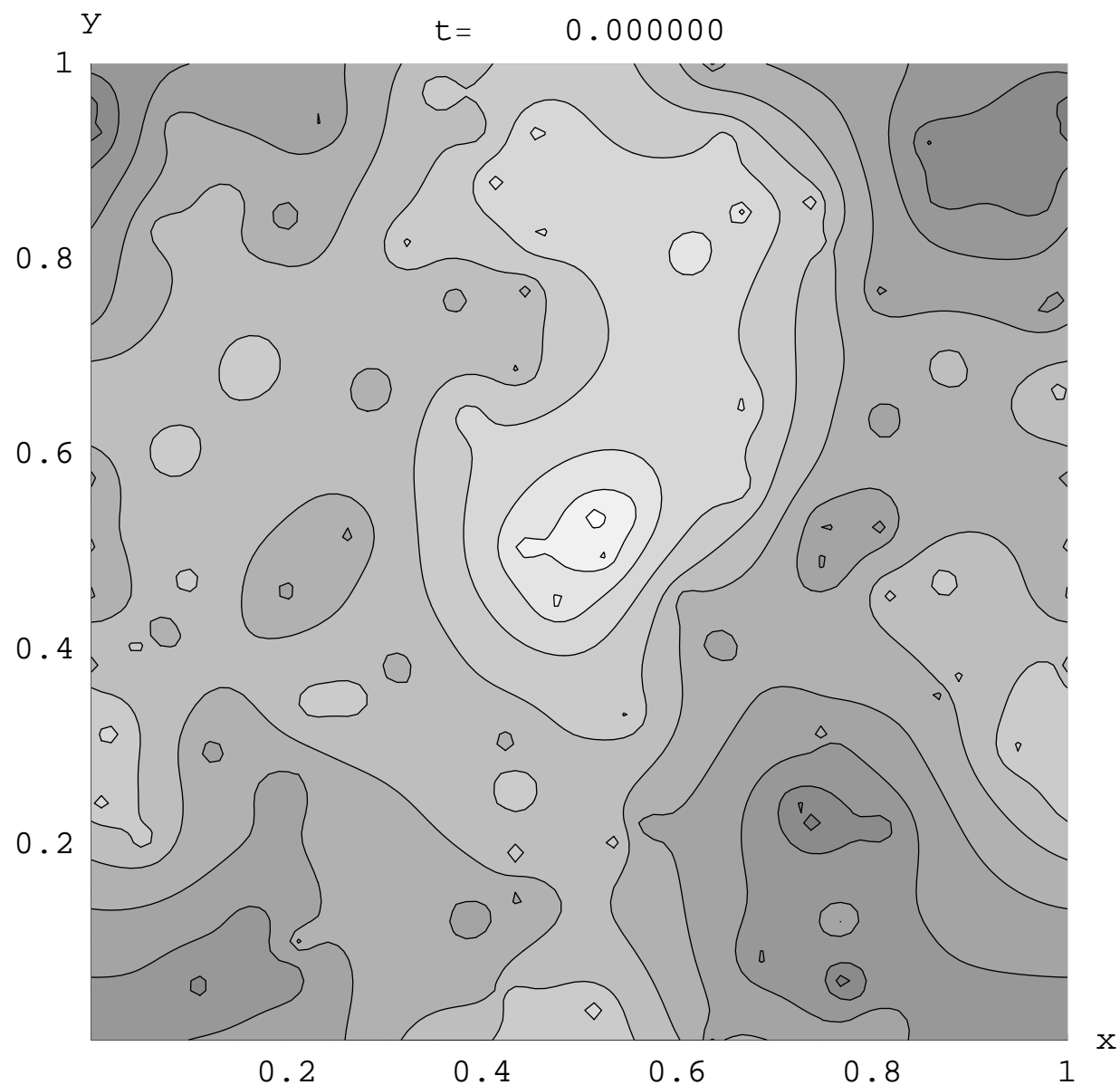


Figure 4c

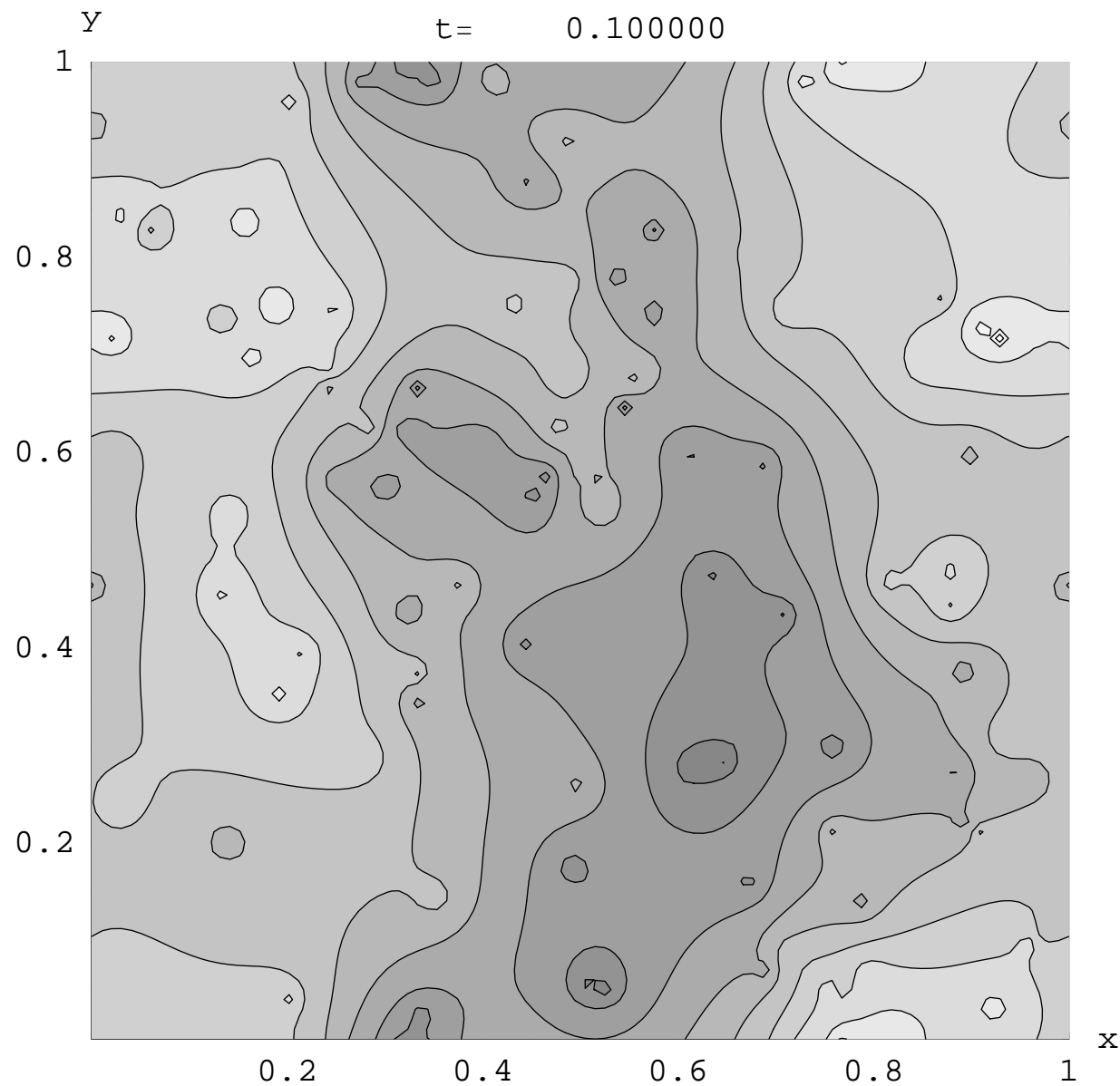


Figure 4d

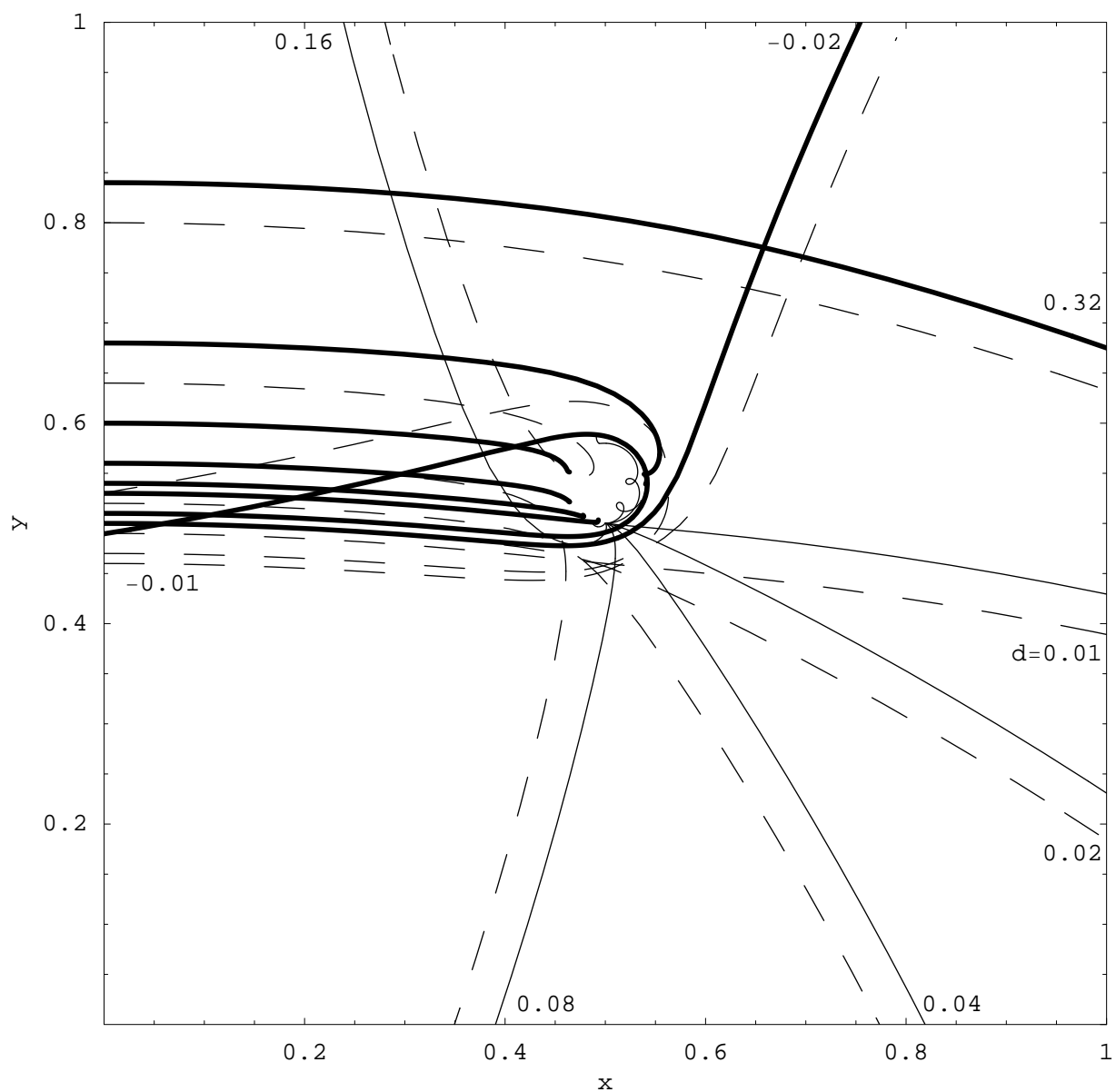


Figure 5

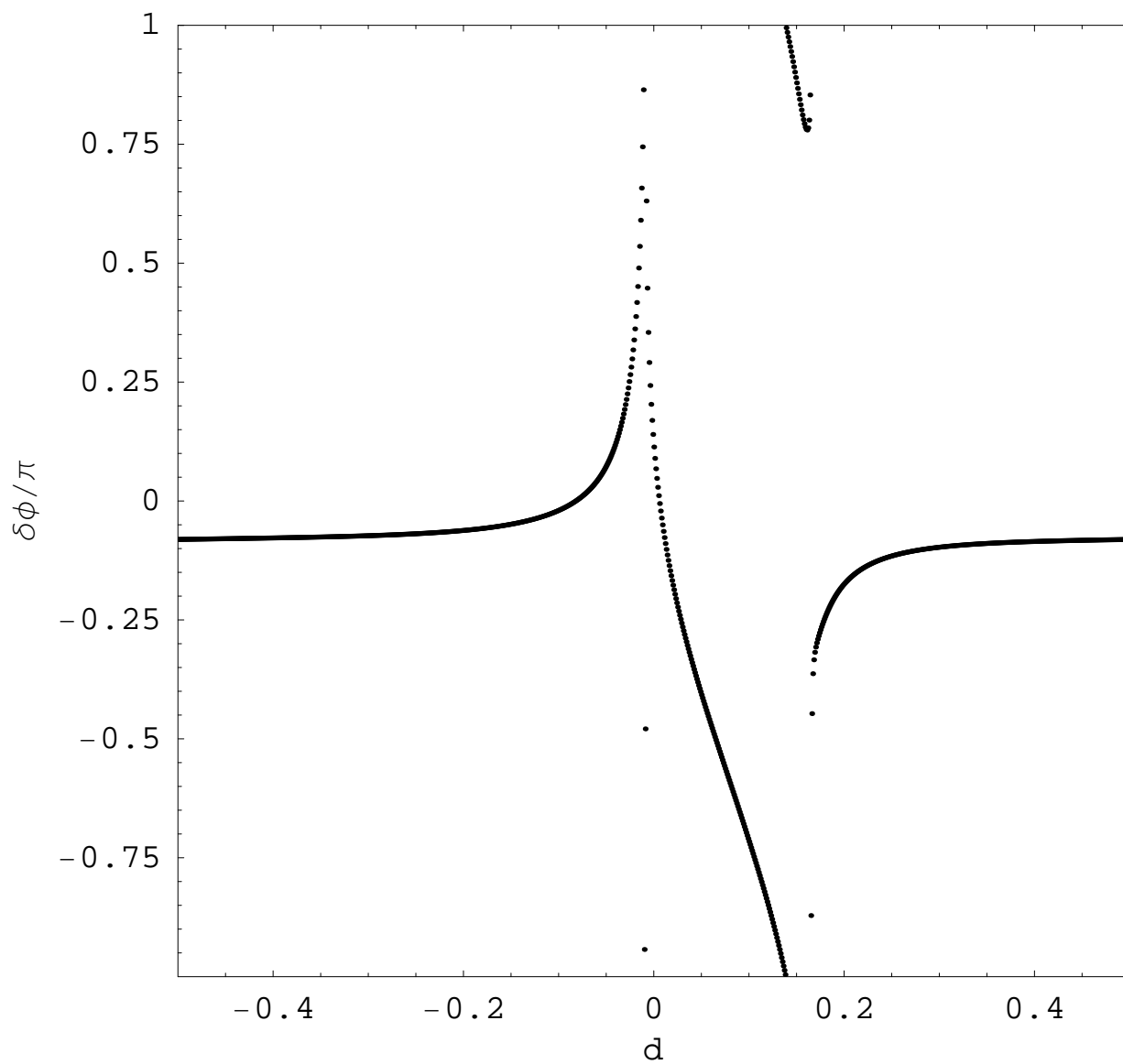


Figure 6

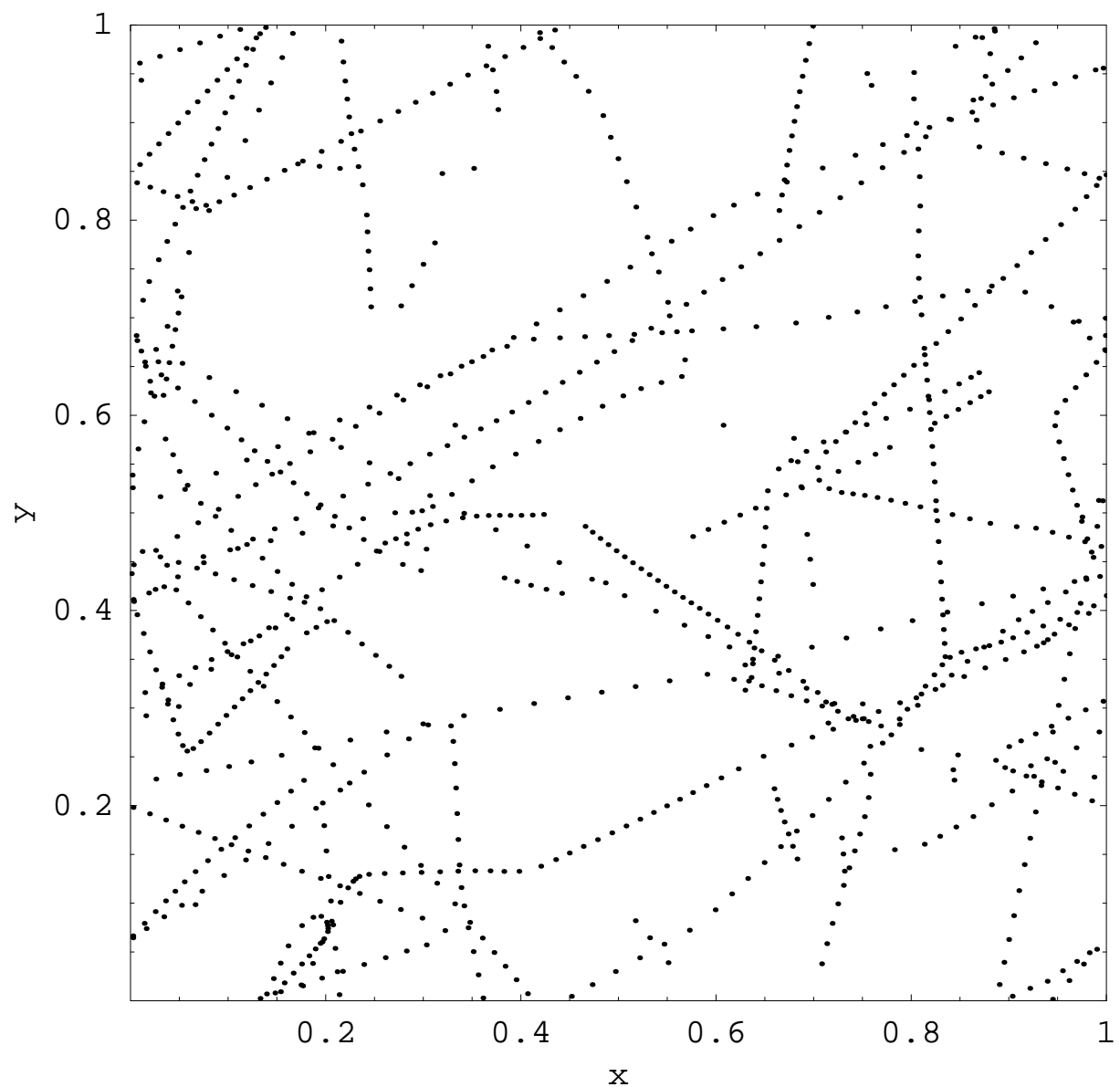


Figure 7

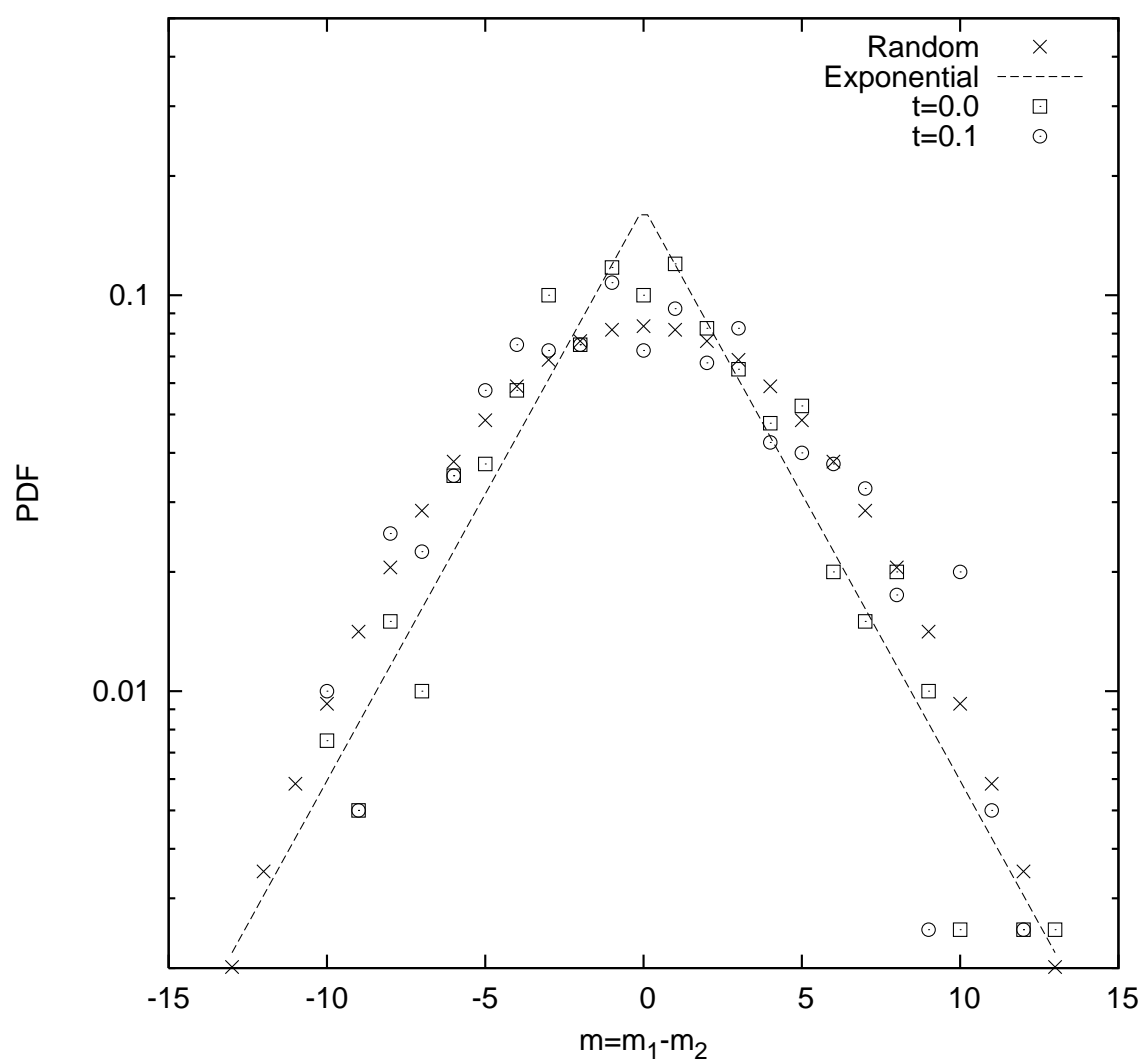


Figure 8